Intermediately bound excitons

1997 J. Phys.: Condens. Matter 9 5355

(http://iopscience.iop.org/0953-8984/9/25/005)

J. Phys.: Condens. Matter **9** (1997) 5355–5370. Printed in the UK PII: S0953-8984(97)80794-1

Intermediately bound excitons

P Dahan†, V Fleurov† and K Kikoin‡

† Beverly and Raymond Sackler Faculty of Exact Sciences, School of Physics and Astronomy, Tel Aviv University, Tel Aviv 69978, Israel

‡ Russian Scientific Centre 'Kurchatov Institute', Moscow 123182, Russia

Received 9 January 1997

Abstract. A possibility of intermediately bound excitons in semiconductors doped with transition metal impurities is considered. These sorts of exciton can appear in hexagonal (wurzite-type) semiconductors due to strong hybridization of the conduction band states and the impurity d states. In tetrahedral (zinc blende) semiconductors this hybridization is strongly suppressed due to a symmetry consideration. It is shown that the exciton hole in ZnS:Ni (zinc blende type) is bound by the Coulomb field of the exciton electron and may be considered within the framework of the hydrogen-like model. As for CdS:Ni (wurzite type) the orthogonalization central cell pseudopotential appears to be the leading attracting potential for the hole. These differences in the binding mechanisms account for striking differences measured experimentally in the structure of the exciton spectra and values of the g-factors of these two presumably similar systems.

1. Introduction

Bound electron–hole pairs, i.e. excitons, are typical excitations of electronic subsystems of semiconductors and molecular crystals. Two types of exciton are usually distinguished. These are Frenkel excitons, strongly localized within an atomic distance and observed mainly in molecular crystals, and Wannier excitons in semiconductors whose localization radius essentially exceeds the lattice spacing and whose wave functions can be described within the framework of the effective mass theory.

Defects and impurities can bind free Wannier excitons. The excitons bound to charged centres are characterized by a rather large localization radius, so these states are well described by the effective mass theory. Neutral isoelectronic impurities are also capable of binding excitons [1]. In this case one of the carriers is trapped by the short-range potential of the impurity and has a smaller localization radius. The second carrier is now attracted by the Coulomb potential of the first one.

Unlike the simple neutral impurities, the isoelectronic transition metal impurities capture one carrier in their electrically active d shell, i.e., in the deep level created by this impurity, and the second carrier is again attracted by the Coulomb potential of the first one. Such bound excitons are observed as lines in the excitation spectra in the low energy onset of the charge transfer band. Involvement of the impurity d shell in formation of the bound exciton is manifested, e.g., in a possibility of multicharge states of the transition metal impurities and in amphoteric behaviour of the excitons [2]. The reaction

$$\mathrm{d}^n + h\nu \Rightarrow [\mathrm{d}^{n+1}, \mathrm{h}]$$

0953-8984/97/255355+16$19.50

produces an acceptor-type exciton while a donor-type exciton is produced by the reaction

$$d^n + h\nu \Rightarrow [d^{n-1}, e].$$

Properties of the excitons bound to transition metal impurities in semiconductors are reviewed in [3, 4].

An idea of intermediately bound excitons when both carriers are captured at intermediate-radius orbitals is empirically formulated in recent experimental studies of exciton luminescence in ZnS and CdS doped by Ni [5] (see also experiments on Cu [6, 7]). Attention was drawn in these papers to the fact that the properties of the excitons bound to Ni impurities behave differently in these two apparently similar semiconductors. The most important differences are the following.

(i) The zero-phonon line in both systems is split into a triplet but with strongly differing g-factors: $g = 0.5$ for ZnS:Ni and $g = 2.26$ for CdS:Ni.

(ii) The excitation spectra of ZnS:Ni are more complicated than those of CdS:Ni.

(iii) The binding energy of the loosely bound carrier is estimated as about 20 meV [8] or 108 meV [5] for ZnS:Ni and its value is found to be $\approx$140 meV for CdS:Ni.

The assumption of different localization radii of excitons in ZnS:Ni and in CdS:Ni gave the authors of [5] the possibility of explaining these features, at least phenomenologically.

The aim of this paper is to present a microscopical theory of excitons intermediately bound to transition metal impurities and to explain the origin of the different properties of the bound excitons in zinc blende and wurzite crystals doped with Ni. The differences listed above will be shown to be connected to the different symmetries of these two materials: zinc blende, ZnS, crystallizes in a tetrahedral lattice (T_d group), whereas CdS has a wurzite type lattice (C_{6v} hexagonal group). The lower symmetry of the crystalline environment of the substitutional Ni impurity in the trigonal CdS versus tetrahedral ZnS results in an essential modification of the wave functions of electrons localized around the Ni impurity and eventually in a transformation of the deeply bound excitons into intermediately bound ones and in partial 'equalizing' of the behaviour of the electron and the hole constituting the bound exciton. This equalization means that, unlike the standard cases of excitons bound to neutral impurities, both bound carriers acquire features of localized deeply bound d states. It will be shown that such equalization can explain anomalous features of the exciton luminescence spectra in CdS:Ni compounds including the change of the exciton g-factor in comparison with ZnS:Ni. A preliminary report on this work was published in [9].

2. Model

The excitons intermediately bound to 3d impurities are similar in many aspects to those deeply bound to usual neutral impurities. Both are characterized by multielectron impurity configurations $[A^{(-)}(d^n + e), h]$ for the acceptor- and $[A^{(+)}(d^n + h), e]$ for the donor-type excitons. Here $A^{(\mp)}$ represents the impurity configuration whose d shell either possesses an extra electron or lacks it. Using the quasiatom model [10] based partially on the formalism of conventional strong-crystal-field theory, the multielectron wave functions of these configurations can be written as

$$\begin{aligned}\Psi_\Gamma^{(ex)}(d^{n-1}, e) &= \hat{A} \sum_{\Gamma'\gamma} C^\Gamma_{\Gamma'\gamma} \Psi_{i\Gamma'}(d^{n-1}) \psi^{(e)}_\gamma \\ \Psi_\Gamma^{(ex)}(d^{n+1}, h) &= \hat{A} \sum_{\Gamma'\gamma} C^\Gamma_{\Gamma'\gamma} \Psi_{i\Gamma'}(d^{n+1}) \psi^{(h)}_\gamma.\end{aligned} \tag{1}$$

Here $C^{\Gamma}_{\Gamma'\gamma}$ are the Clebsch–Gordan coefficients realizing the direct product Γ of the multi-electron wave functions corresponding to the $\Gamma'(\mathrm{d}^{n\pm1})$ irreducible representations and the loosely bound γ electron or hole. $\hat{A}$ is the antisymmetrization operator.

The Ni impurity may form an acceptor-type bound exciton, $[\mathrm{d}^{n+1}, \mathrm{h}]$ in ZnS and CdS [3, 5] with the binding energy defined as

$$E_{bex} = E(\mathrm{d}^{(n+1)}, \mathrm{h}) - E(\mathrm{d}^{(n)}). \tag{2}$$

The single-electron functions used to construct the multielectron functions (2) are eigenfunctions of the impurity Hamiltonian

$$H_e = \hat{T} + V_d(\boldsymbol{r} - \boldsymbol{R}_0) + U'(\boldsymbol{r} - \boldsymbol{R}_0) + U_1\{\Delta\rho(\boldsymbol{r})\} \tag{3}$$

where $\hat{T}$ is the electron kinetic energy operator, $V_d(\boldsymbol{r} - \boldsymbol{R}_0)$ is the substitutional impurity potential, and $U'(\boldsymbol{r} - \boldsymbol{R}_0)$ is the lattice crystal field potential acting on the impurity. $U_1\{\Delta\rho(\boldsymbol{r})\}$ is the potential due to the distorted valence electron density. The multielectron wave function $\Psi_{\Gamma'}$ of the d shell is treated using the conventional Russel–Saunders scheme.

The hole wave function $\psi^{(h)}_{i\gamma}$ is an eigenfunction of the Hamiltonian $-H_v(\boldsymbol{r})$ of the valence band with one electron removed. As a result, the acceptor bound exciton can be described by the $(n+2)$-particle wave function which corresponds to the configuration $[\mathrm{d}^{(n+1)}, \mathrm{h}]$ of the impurity ion. After excluding the 'core' part of the impurity pseudoion, d^n, the general Schrödinger equation is reduced to the following two-particle equation:

$$[H_e(\boldsymbol{r}_1) - H_v(\boldsymbol{r}_2) + U(\boldsymbol{r}_1 - \boldsymbol{r}_2) - E^{ex}_I]\hat{A}\psi^{(n+1)}_{i\Gamma'}(\boldsymbol{r}_1)\psi^{(h)}_{i\gamma}(\boldsymbol{r}_2) = 0 \tag{4}$$

where the exciton energy is just the difference

$$E^{ex}_I = E_V(N-1) + E_{i\Gamma'}(\mathrm{d}^{n+1}) - E_V(N) - E_{i\Gamma}(\mathrm{d}^n) \tag{5}$$

of the total energies of the system with and without the exciton. It is to be determined from equation (5). The total energy of the system with the exciton includes the energy $E_V(N)$ of the valence band completely filled by N electrons and the energy $E_{i\Gamma}(\mathrm{d}^n)$ of the n-electron ground state of the neutral impurity atom. A bound exciton is formed by a hole in the valence band with the energy $E_V(N-1)$ and by the $(n+1)$th electron in the potential $U_{d\gamma}(\boldsymbol{r})$ created by the d^n core of the impurity d shell. The energy of the latter becomes $E_{i\Gamma'}(\mathrm{d}^{n+1})$ whereas its $(n+1)$-electron wave function is $\psi^{(n+1)}_{i\Gamma}(\boldsymbol{r})$. $U(\boldsymbol{r}_1 - \boldsymbol{r}_2) = e^2/\varepsilon|\boldsymbol{r}_1 - \boldsymbol{r}_2|$ is the Coulomb electron–hole interaction.

Since the electron wave function even in an intermediate-radius exciton is more localized than the hole wave function, first the single-electron Schrödinger equation

$$(H_e + E_{i\Gamma'}(\mathrm{d}^{(n)}) - E)\psi^{(n+1)}_{i\gamma}(\boldsymbol{r}) = 0 \tag{6}$$

is considered, the electron–hole Coulomb interaction, $U(\boldsymbol{r}_1 - \boldsymbol{r}_2)$, being neglected. This equation determines the position of the level $E^{(n+1)}_{i\tilde{\gamma}}$ of the $(n+1)$th bound electron and its wave function $\psi^{(n+1)}_{i\tilde{\gamma}}(\boldsymbol{r})$.

Similarly, the equation

$$\left[-\left(\hat{T} + \sum_j U'(\boldsymbol{r} - \boldsymbol{R}_j) + U_{d\gamma}(\boldsymbol{r})\right) - U(\boldsymbol{r}) - E_h\right]\psi^{(h)}_{i\gamma}(\boldsymbol{r}) = 0 \tag{7}$$

can be derived from equation (4) for the hole wave function, where $E_h = E - E^{(n+1)}_{i\tilde{\gamma}}$. The Coulomb potential $U(\boldsymbol{r})$ arises due to the interaction between the hole and the $(n+1)$th electron in the d shell of the impurity ion.

In the case of a conventional isoelectronic d impurity, equations (6) and (7) result in a standard bound exciton picture described, e.g., in [1, 11, 12]. Many of their features were

analysed in [2, 13], but the possibility of forming a pair with comparable radii of electron and hole in a hexagonal host crystal needs a special consideration, so this mechanism should be revisited. A special attention will be paid to a short-range central cell pseudopotential which will be shown to play an important part in the formation of a bound exciton in the CdS host. For this sake we consider the properties of an electron and hole bound by a Ni impurity in ZnS and CdS more carefully. The neutral Ni impurity in II–VI semiconductors has a d^8 configuration, thus we start with $n = 8$ in equations (2) and (4)–(6). A negatively charged nickel ion, $Ni^{(-)}(d^9)$, produces localized states in the upper part of the forbidden energy gap in the majority of II–VI compounds. The level energy $E_i(0/-)$ is found to be $\approx$1 eV under the bottom of the conduction band of ZnS:Ni and very close to the bottom of the conduction band in CdS:Ni. This ninth electron plays the role of a relatively tightly bound carrier which creates an attractive potential for a more or less loosely bound hole. In the two following sections we will consider the difference between degrees of localization of these two partners in zinc blende and wurzite host crystals.

3. The tightly bound electron

It is known from the general theory of 3d impurities in semiconductors [15–18] that the shape of the impurity wave function and the position of the impurity deep level are determined largely by the covalent hybridization of the impurity d orbitals with the band states of the host material (a detailed discussion of the problem is presented in the review [14] and in the book [4]). To find the solution of equation (6) one should use the set of functions $\{\tilde{\psi}_{\boldsymbol{k}a\sigma}, \psi_{\bar{\gamma}\mu}\}$ in the expansion of the localized electron wave function. This set includes the wave functions, $\psi_{\bar{\gamma}\mu}$, of the atomic d electrons in the local crystal field along with the Bloch functions, which should be orthogonalized to the d electron wave functions

$$\tilde{\psi}_{\boldsymbol{k}a\sigma} = \psi_{\boldsymbol{k}a\sigma} - \sum_{\gamma\mu} \langle \gamma\mu | \boldsymbol{k}a\sigma \rangle \psi_{\gamma\mu}.$$

The state of the ninth electron in the $Ni^{(-)}$ d shell corresponds to a t_2 representation ($\bar{\gamma} = \Gamma_5$), and the electron states of the Γ_5 representation in the heavy-hole band give the dominant contribution to the hybridization. Then the energy level $\varepsilon^{(9)}_{\Gamma_5}$ of the electron in the d^9 shell is given by the equation

$$E_{i\Gamma_5} = \varepsilon^{(n+1)}_{\Gamma_5} + \Delta U + M_v(E_{i\Gamma_5}) \tag{8}$$

where the potential part of the impurity scattering is omitted in comparison with the resonant scattering by the d level of the unfilled impurity shell. Here

$$M_v(E_{i\Gamma_5}) = \sum_{\boldsymbol{k}} \frac{|V_{\Gamma_5 v}(\boldsymbol{k})|^2}{E_{i\Gamma_5} - \varepsilon_{v\boldsymbol{k}}}. \tag{9}$$

The ninth electron ionization energy is defined as

$$\varepsilon^{(9)}_{\Gamma_5} = E(d^9) - E(d^8)$$

ΔU is the renormalization due to the response of the host states to the excess impurity charge [15], and

$$V_{\Gamma_5 v}(\boldsymbol{k}) = \langle \tilde{\boldsymbol{k}v} | U'(\boldsymbol{r} - \boldsymbol{R}_0) | \Gamma_5 \mu \rangle \tag{10}$$

is the hybridization matrix element responsible for mixing of atomic and band states in the above basis.

The wave function of the ninth electron consists of a localized 'core' and an extended 'Bloch tail',

$$\psi^{(9)}_{i\Gamma_5} = \left[1\Big/\sqrt{(1+\tilde{M}'_{v\Gamma_5})}\right]\left[\psi_{dt_2} + \sqrt{\tilde{M}'_{v\Gamma_5}}\psi_{bt_2}\right] \tag{11}$$

where

$$M'_{v\gamma} = -\mathrm{d}M_v(E_{i\gamma})/\mathrm{d}E_{i\gamma}. \tag{12}$$

Here ψ_{dt_2} is the atomic d-electron wave function, and the properties of the Bloch tail $\psi_{bt_2}(\boldsymbol{r})$ are described in the appendix.

First, we consider the zinc-blende-type crystals of T_d point symmetry. It is known [4, 14] that the states in the lower part of the conduction band only weakly influence the electronic structure of 3d impurities in zinc blende crystals since these states are formed predominantly by the s orbitals, which can form only nonbonding states with the transition metal d orbitals. As a result the hybridization matrix elements (10) are proportional to the absolute value k of the wave vector near the bottom of the conduction band. Neglecting this term in $\psi_{bt_2}(\boldsymbol{r})$ and keeping in mind that the heavy-hole band gives the leading contribution among the valence bands, one can approximately write the impurity wave function as an antibonding combination of the atomic d function, ψ_d, and the Bloch tail, φ_p, of p symmetry.

$$\psi_{i\Gamma_5} \simeq \left[1\Big/\sqrt{1+M'_{v\Gamma_5}}\right]\left[\psi_d - \sqrt{M'_{v\Gamma_5}}\varphi_p\right]. \tag{13}$$

Thus the impurity level position should be counted from the top of the valence band. In this sense the level in the upper part of the forbidden energy gap appears to be very deep. This means that the Bloch tail φ_p of the wave function (13) is rather short range and it has a rather small weight in the impurity wave function (13) as compared to that of the atomic d function, ψ_d. This weight is proportional to the factor $M'_{v\Gamma_5}$ (shown in figure 1) which decreases with increasing distance from the top of the valence band.

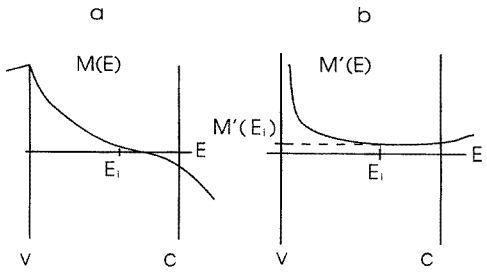

Figure 1. A schematic representation of the energy dependence of the function $M(E)$ (9) (a) and its derivative $M'(E)$ (12) (b) in a zinc-blende-type crystal. One can see that both the function $M(E)$ and its derivative $M'(E)$ are smooth near the conduction band edge since hybridization of d states with the conduction band states is symmetry forbidden. As a result a possible influence of the van Hove edge singularity is suppressed.

Quite different is the situation with the same level in a hexagonal environment of the wurzite lattice. Both the states at the top of the valence band and at the bottom of the conduction band transform according to the Γ_7 representation of the crystal group C_{6v}. When introducing an impurity in a cation position the symmetry group is lowered to C_{3v} and this group is used to classify the localized states. Then the irreducible representation Γ_4 of the C_{3v} point group takes the place of the representation Γ_7 of the C_{6v} group. As

a result the wave function of the ninth electron in the d shell of a charged $Ni^{(-)}(d^9)$ ion, which transforms according to the representation Γ_4, hybridizes strongly with both valence and conduction band states so that both matrix elements $\tilde{V}_{\Gamma_4 c}$ and $\tilde{V}_{\Gamma_4 v} \sim$ constant at $k \to 0$.

Then the important parameter for comparison of the valence and conduction band contributions to the Bloch tail $\psi_{b\Gamma_4}$ is the energy distance between the impurity level and the corresponding band edges. In CdS:Ni the impurity level $E^{(9)}_{i\Gamma_4}$ is very deep with respect to the valence band and is shallow with respect to the conduction band. Moreover, the nonzero value of $V_{\Gamma_7 c}(k = 0)$ leads to a cusp of the Hilbert transform $M_v(\varepsilon_c)$ determined by an equation similar to equation (9) and, as a result, to a singularity of its derivative $M'_{c\Gamma_4}(E \to \varepsilon_c) \to \infty$ (see figure 2). This makes the contribution of the conduction band dominant, and the impurity function can be written as a bonding combination

$$\psi_{i\Gamma_4} \simeq \left[1 \Big/ \sqrt{(1 + M'_{c\Gamma_4})}\right]\left[\psi_d + \sqrt{M'_{c\Gamma_4}}\varphi_s\right]. \tag{14}$$

Thus the Bloch tail dominates in the wave function of the ninth electron in the unfilled d shell of impurity pseudoion $Ni^{(-)}(\tilde{d}^9)$, and the impurity wave function in the wurzite crystal $CdS:Ni^{(-)}$ appears to be much more extended than that in the tetrahedral $ZnS:Ni^{(-)}$ crystal.

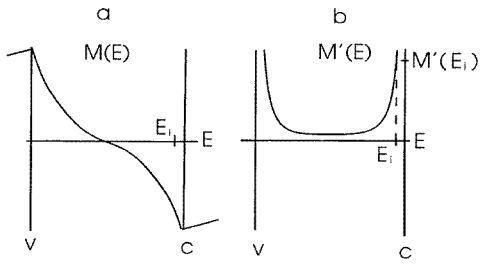

Figure 2. A schematic representation of the energy dependence of the function $M(E)$ (9) (a) and its derivative $M'(E)$ (12) (b) in a wurzite-type crystal. One can see that the function $M(E)$ has a cusp which becomes a divergency of the function $M'(E)$, which is caused by the van Hove singularity near the conduction band edge. This sort of behaviour shows up due to the fact that the symmetry ban existing in the zinc-blende-type crystals is now lifted.

4. Loosely bound hole

Now we turn to calculation of the hole eigenenergy, $E^{(h)}_i$, and its wave function, $\psi^{(h)}_{i\gamma}$. Usually the second partner in an electron–hole pair bound to a simple isoelectronic impurity is well described by assuming a point charge potential. The effective mass approximation with central cell corrections [19] is then applied. The latter takes into account the short-range non-Coulomb potential of the impurity core. Since the shell of the transition metal impurity is strongly distorted due to hybridization with band states [3, 4], the central cell corrections are expected to be of much more importance in our case. This section discusses the mechanisms of the hole binding which may be either due to the Coulomb long-range potential or due to the short-range interaction depending on the symmetry of the host crystal.

Usually a loosely bound state is orthogonalized to the core states of the impurity which results in a contribution to the impurity potential known as central cell corrections [20]. In the case of a bound exciton the hole wave function should be orthogonalized to the wave

function of its electron counterpart (to the swollen state of the ninth electron in the case of an Ni impurity) as well. Therefore the hole wave function is looked for in the form

$$\psi_{i\gamma}^{(h)} = A_\gamma^{-1/2}\left[\sum_k F_v^\gamma(\boldsymbol{k})\tilde{\psi}_{\boldsymbol{k}v}(\boldsymbol{r}) + F_d^\gamma \psi_{i\gamma}\right]. \tag{15}$$

The first term in this expansion is the Bloch tail expanded over the Bloch functions

$$\tilde{\psi}_{\boldsymbol{k}v} = \psi_{\boldsymbol{k}v} - \sum_\lambda \langle \tilde{\mathrm{d}\lambda}|\boldsymbol{k}v\rangle \psi_{i\lambda}. \tag{16}$$

orthogonalized to all states of the $\mathrm{Ni}^{(-)}(\tilde{\mathrm{d}}^9)$ pseudoion (the set λ includes the γ state of the last outer electron). To find the coefficients F_γ one should repeat the Harrison procedure [21] for the 'resonance' pseudopotential of noble and transition metals. Inserting (15) in equation (7) one readily finds

$$F_d^\gamma = -\frac{\langle \tilde{\mathrm{d}\gamma}|U_d|\psi_{b\gamma\mu}\rangle}{(E_h + E_{i\Gamma})}. \tag{17}$$

The factor A_γ can be found from the normalization condition for the function (15). Then, in close analogy with the case of the deep resonance state [17] we find the effective Schrödinger equation for the band part of the loosely bound hole wave function $\psi_{b\gamma}$

$$\left[-\left(\hat{T} + \sum_j U(\boldsymbol{r} - \boldsymbol{R}_j)\right) + U_c(\boldsymbol{r} - \boldsymbol{R}_0) - \Delta\tilde{U}_{cc} + \hat{U}_\gamma^{res} - E_h\right]\psi_{b\gamma}(\boldsymbol{r} - \boldsymbol{R}_0) = 0 \tag{18}$$

where

$$\hat{U}_\gamma^{res}\psi_{b\gamma}(\boldsymbol{r} - \boldsymbol{R}_0) = \int U_\gamma^{res}(\boldsymbol{r}, \boldsymbol{r}')\psi_{b\gamma}(\boldsymbol{r}' - \boldsymbol{R}_0)\,\mathrm{d}^3r'$$

and

$$U_\gamma^{res}(\boldsymbol{r}, \boldsymbol{r}') = \sum_{\gamma'} \frac{W(\boldsymbol{r})|\tilde{\mathrm{d}\gamma'}\rangle\langle\tilde{\mathrm{d}\gamma'}|W(\boldsymbol{r}')}{E_h + E_{i\gamma'}}.$$

Here the potential $U_{d\gamma}(\boldsymbol{r})$ of the Ni impurity with an excess electron is represented as a sum of the Coulomb potential $U_c(\boldsymbol{r} - \boldsymbol{R}_0)$ and the short-range pseudopotential $\Delta\tilde{U}_{cc}$ which has the standard form as described in [21]. Here $W(\boldsymbol{r}) = U'(\boldsymbol{r} - \boldsymbol{R}_0) + U_1\{\Delta\rho(\boldsymbol{r})\}$ is the crystal field potential in (3) due to the field of the host ions and of the distorted valence electron density. The resonance potential $\hat{U}_\gamma^{res}$ and its role in the formation of bound excitons was discussed in [3].

Inserting the orthogonalized Bloch functions (16) into (18), one arrives at the system of linear equations for the coefficients $F_v^\gamma(\boldsymbol{k})$ determining the wave function (15),

$$[E_{v\boldsymbol{k}} - E_h]F_v^\gamma(\boldsymbol{k}) - \sum_{\boldsymbol{k}'v'}[U_{vv'}^s(\boldsymbol{k}, \boldsymbol{k}') + U_{\gamma,vv'}^{cc}(\boldsymbol{k}, \boldsymbol{k}') - U_{\gamma,vv'}^{res}(\boldsymbol{k}, \boldsymbol{k}')]F_{\boldsymbol{k}'v'}^\gamma = 0. \tag{19}$$

Here $U_{vv'}^s(\boldsymbol{k}, \boldsymbol{k}')$ are the matrix elements of the Coulomb potential and $U_{\gamma,vv'}^{cc}(\boldsymbol{k}, \boldsymbol{k}')$ and $U_{\gamma,vv'}^{res}(\boldsymbol{k}, \boldsymbol{k}')$ are those of the short-range and the resonance scattering potentials respectively. One can neglect as usual the off-diagonal matrix elements of the Coulomb potential, by assuming $U_{vv'}^s(\boldsymbol{k}, \boldsymbol{k}') = U_v^s(\boldsymbol{k}, \boldsymbol{k}')\delta_{vv'}$. It should be also taken into account that this potential is created by the charge of the exciton electron bound to the impurity with a finite localization radius. The corresponding corrections were discussed in [2], where it was shown that they can make the hole level more shallow provided the radius of swollen electron orbital $\tilde{\mathrm{d}}_\gamma$ is comparable with the radius of the hydrogen-like bound hole.

The term

$$U^{cc}_{\gamma,\alpha\alpha'} = \langle\alpha|U_s|\alpha'\rangle + S_{\alpha\gamma}(E_{i\gamma} - E_h)S^*_{\gamma\alpha'} + V_{\alpha\gamma}S^*_{\gamma\alpha'} + S_{\alpha\gamma}V^*_{\gamma\alpha'} \tag{20}$$

is just a conventional short-range impurity pseudopotential (see, e.g., [21]). Here

$$\langle\alpha|U_s|\alpha'\rangle = \langle\alpha|(V_d(\boldsymbol{r} - \boldsymbol{R}_0) - V_h(\boldsymbol{r} - \boldsymbol{R}_0)|\alpha'\rangle$$

is a matrix element of the substitutional potential which arises due to the difference between the core states of the impurity and host ion; $|\alpha\rangle = |\boldsymbol{k}a\sigma\rangle$, $S_{\alpha\gamma} = \langle\alpha|\tilde{\mathrm{d}}\gamma\rangle$; $V_{\alpha\gamma} = \langle\alpha|U_d|\tilde{\mathrm{d}}\gamma\rangle$ are the nonorthogonality and hybridization integrals.

The contributions of the orthogonalization corrections to the central cell potential in zinc blende and wurzite hosts are different due to the different behaviour of the ninth electron of the Ni ions in corresponding crystalline environments. The hole wave function is orthogonalized to all electron wave functions of the impurity, given by equation (13) in the zinc blende ZnS and (14) in the wurzite type host CdS, respectively. Substituting these into equation (20) one obtains that the contribution due to the Bloch tails of the functions (13) and (14) has the form

$$U^{cc}_{\gamma,\alpha\alpha'} \approx \left(\frac{M'_{a\gamma}}{1 + M'_{a\gamma}}\right)U_{d,aa'}(\boldsymbol{k}, \boldsymbol{k}') \tag{21}$$

where

$$U_{d,aa'}(\boldsymbol{k}, \boldsymbol{k}') = \langle\boldsymbol{k}a|\Delta E\,\hat{P}_\gamma + U_d\hat{P}_\gamma + \hat{P}_\gamma U_d|\boldsymbol{k}'a'\rangle$$

with $\hat{P}_\gamma = |\varphi_\gamma\rangle\langle\varphi_\gamma|$ being the projection operator and φ_γ being the Bloch tail of the impurity wave functions (13) and (14); $\Delta E = E_{i\gamma} - E_h$. Excitons bound to transition metal impurities with a deep d state in a host with the $\mathrm{T_d}$ ($\gamma = \Gamma_5$) symmetry were studied in [2], and it was found that both pseudopotential and resonance contributions are small if the electron wave function is sufficiently localized. Then $M'_{a\Gamma} < 1$ and the term (20) is of no importance for the formation of the hole bound state. The bound electron charge can be also considered as nearly pointlike and the conventional effective mass approximation with the central cell corrections is applicable to the description of the bound hole in ZnS:Ni.

The situation in a wurzite-type crystal ($\mathrm{C_{3v}}$ point group, $\gamma = \Gamma_4$) appears to be quite different. The pseudopotential (21) in CdS:Ni is strongly enhanced due to the lift of the symmetry ban for the hybridization, discussed in the previous section, which results in $M'_{a\Gamma_4} \gg 1$. Now this pseudopotential is responsible for the hole binding whereas the Coulomb potential (decreased due to smearing of the electron charge in the centre) can lead only to small corrections.

It is worthwhile to compare this situation with the results of Perel' and Yassiyevich [22], who have considered formation of deep levels by a short-range impurity potential. Although the problems are very similar, two important differences are to be mentioned. The impurity potential considered in [22] transforms according to the Γ_1 irreducible representation and does not introduce any symmetry restrictions. The structure and symmetry features of the levels created by such a potential are controlled by the host band structure. In our case the impurity potential transforms according to the Γ_4 (Γ_7) irreducible representation and has properties of the corresponding projection operator. This means that only Γ_4 band states participate in the formation of the impurity levels. As a result the classification of the levels to be obtained is at variance from those of [22].

The second difference is connected with the fact that [22] considers neutral impurities whereas we deal with a charged impurity. However the corresponding Coulomb potential is relatively weak and may introduce only small perturbations without changing the symmetry properties of the levels. The same relates also to the resonance term in equation (18).

The conclusion is that, provided this potential is strong enough, the hole of the bound exciton in CdS:Ni can be described as follows.

(i) The short-range potential does not interact with the Bloch states of the topmost Γ_9 band and corresponding hydrogen-like shallow levels are formed by the Coulomb part of the impurity potential.

(ii) The short-range pseudopotential splits a bound hole state from the subsequent Γ_7 bands with energies which may be essentially deeper than that of the hydrogen-like states.

(iii) This level turns out to be the lowest bound hole state, and it has smaller effective radius than that of the hydrogen-like state.

Other properties of this ground state and estimates of its energy will be discussed below.

4.1. The hole binding energy

It is assumed here that in CdS:Ni it is the short-range pseudopotential (20) which forms the bound hole states. The projection properties of this pseudopotential determine the symmetry properties of the hole wave function which transforms according to the irreducible transformation Γ_7 of the C_{6v} group (which corresponds to the representation Γ_4 of the C_{3v} group). The other contributions such as those of the Coulomb potential and the resonant scattering do not change the symmetry properties of the hole state and may introduce a relatively weak perturbation. Therefore it is a good approximation to look for the coefficients $F_v^\gamma(\boldsymbol{k})$ as satisfying the equation

$$F_v^\gamma(\boldsymbol{k}) - \frac{1}{E_{v\boldsymbol{k}} - E_h} \frac{M'_{c\Gamma}}{1 + M'_{c\Gamma}} \sum_{\boldsymbol{k}'v'} U_{d,vv'}(\boldsymbol{k}, \boldsymbol{k}') F_{v'}^\gamma(\boldsymbol{k}') = 0. \tag{22}$$

Now the fact that the short-range potential (20) contains factorizable terms is explicitly used. Introducing two auxiliary variables

$$\begin{aligned} A_S &= \sum_{\boldsymbol{k}v} S_{\boldsymbol{k}v\Gamma_7} F_{\boldsymbol{k}v}^\gamma \\ A_V &= \sum_{\boldsymbol{k}v} V_{\boldsymbol{k}v\Gamma_7} F_{\boldsymbol{k}v}^\gamma \end{aligned} \tag{23}$$

we find the system of equations

$$\begin{aligned} &A_S[1 - B_{SS}\,\Delta E - B_{SV}] - A_V B_{SS} = 0 \\ &-A_S[\Delta E\, B_{SV} + B_{VV}] + A_V[1 - B_{SV}] = 0 \end{aligned} \tag{24}$$

where

$$\begin{aligned} B_{SS}(E_h) &= \frac{M'_{c\Gamma}}{1 + M'_{c\Gamma}} \sum_{\boldsymbol{k}v} \frac{1}{E_{v\boldsymbol{k}} - E_h} S^*_{\boldsymbol{k}v\Gamma_7} S_{\boldsymbol{k}v\Gamma_7} \\ B_{SV}(E_h) = B_{VS}(E_h) &= \frac{M'_{c\Gamma}}{1 + M'_{c\Gamma}} \sum_{\boldsymbol{k}v} \frac{1}{E_{v\boldsymbol{k}} - E_h} S^*_{\boldsymbol{k}v\Gamma_7} V_{\boldsymbol{k}v\Gamma_7} \\ B_{VV}(E_h) &= \frac{M'_{c\Gamma}}{1 + M'_{c\Gamma}} \sum_{\boldsymbol{k}v} \frac{1}{E_{v\boldsymbol{k}} - E_h} V^*_{\boldsymbol{k}v\Gamma_7} V_{\boldsymbol{k}v\Gamma_7}. \end{aligned} \tag{25}$$

One can easily check that the quantities (23) and (25) are real.

The set of equations (24) has nonzero solutions if

$$[1 - B_{SV}(E_h)]^2 - B_{SS}(E_h)[\Delta E + B_{VV}(E_h)] = 0 \tag{26}$$

which is the equation for the hole binding energy E_h. The simplifying approximation

$$V_{\boldsymbol{k}v} = V S_{\boldsymbol{k}v}$$

with V being a parameter characterizing the impurity potential, allows one to rewrite equation (26) in the form

$$B_{SS}(E_h) = 1/(2V + \Delta E) \tag{27}$$

which is standard for a Koster–Slater type of problem (graphical analysis of this sort of equations for the case of zinc blende semiconductors can be found, e.g., in [4]).

Equation (27) may have a solution, meaning a localized level in the forbidden energy gap for strong enough scattering potential on its right-hand side. The value of the function $B_{SS}(E_h)$ is essentially controlled by the parameter $M'_{c\Gamma}$. The latter reflects the share of the Bloch tail in the impurity electron wave function (see the discussion in the previous section). This part is small in ZnS:Ni ($M'_{c\Gamma} < 1$) and large in CdS:Ni ($M'_{c\Gamma} \gg 1$). Direct estimates show that according to equation (27) Ni may produce localized levels in the forbidden energy gap of CdS and no levels would appear in ZnS:Ni due to this short-range pseudopotential alone. If one, however, recollects the contribution of the electron–hole interaction to the binding energy, the results can be summarized as follows. Ni(d^9) in the tetrahedral ZnS attracts a hole by its Coulomb potential and creates a series of hydrogen-like levels which may be only slightly corrected by the short-range part of the potential. In contrast, the short-range potential of Ni(d^9) in the hexagonal CdS is rather strong and creates a single hole level of Γ_4 symmetry which may be corrected by the Coulomb interaction.

4.2. The hole wave function

The coefficients F_v^γ which determine the behaviour of the hole wave function (15) can be written as

$$F_v^\gamma(\boldsymbol{k}) = \frac{S_{\boldsymbol{k}v\Gamma_7}}{E_{v\boldsymbol{k}} - E_h} a_\gamma \tag{28}$$

where the parameter a_γ should be found from the normalization condition for the pseudowave function (see equation (22)). As a result

$$F_v^\gamma(\boldsymbol{k}) = \frac{S_{\boldsymbol{k}v\Gamma_7}}{E_{v\boldsymbol{k}} - E_h} \frac{1}{\sqrt{M'_s}} \tag{29}$$

where

$$M'_s = \sum_{\boldsymbol{k}'v'} \frac{|S_{\Gamma_7\boldsymbol{k}'v'}|^2}{(E_{v\boldsymbol{k}} - E_h)^2}. \tag{30}$$

Adding the core part $\psi_{d\gamma}$, the normalized hole wave function (15) has the form

$$\psi^{(h)}_{i\Gamma_4} = \frac{1}{\sqrt{1 + |F_d^\gamma|^2}} \left[\frac{1}{\sqrt{M'_s}} \sum_{\boldsymbol{k}a} \frac{S_{\Gamma_7\boldsymbol{k}a}}{E_{a\boldsymbol{k}} - E_h} \tilde{\psi}_{\boldsymbol{k}v}(\boldsymbol{r}) + F_d^\gamma \psi_{i\gamma'} \right] \tag{31}$$

where

$$F_d^{\Gamma_4} = \frac{\langle i\Gamma_4 | W | \psi_b \rangle}{E_{i\Gamma_4} + E_h}.$$

Finally the bound exciton wave function (1) reads

$$\Psi^{(ex)}_\Gamma(\tilde{\mathrm{d}}^1_+, \mathrm{h}) = \hat{A} \sum_{\Gamma'\lambda} C^\Gamma_{\Gamma'\lambda} \psi_{i\Gamma'}(\boldsymbol{r}_1) \psi^{(h)}_\lambda(\boldsymbol{r}_2) \tag{32}$$

($\lambda = \Gamma_4$). Thus we see that the hole wave function has acquired a 'core' part $\psi_{d\gamma}$ due to the resonance mechanism, so the hole state has a structure similar to that of its electron counterpart (14) in the bound exciton state. The contribution of the Bloch tail to the electron wave function (14) and that of the d core to the hole wave function are controlled by the factors $M'_{c\Gamma_4}$ and $|F_d^{\gamma_4}|^2$, respectively. If there are some special reasons for enhancement of these coefficients, then the 'equalization' of the electron and hole wave functions mentioned above can occur. It is seen now that swelling of the electron component (large $M'_{c\gamma_4}$) results in strong orthogonalization corrections to the hole wave function (large $|F_d^{\Gamma_4}|^2$), and the ultimate source of these two effects is the anomalously strong hybridization of the $d\Gamma_4$ states with the conduction band states which have the same symmetry.

5. Magneto-optics of bound excitons

This section presents a comparison of various experimental observations with the predictions of the model outlined above.

5.1. The g-factor

The magneto-optics of Ni-bound shallow states is controlled by the value of the effective g-factor in the Zeeman interaction

$$H_z = \mu_0[g_e \boldsymbol{S}_e \cdot \boldsymbol{H} + g_h \boldsymbol{S}_h \cdot \boldsymbol{H}]. \tag{33}$$

Here $\boldsymbol{S}_h$ and $\boldsymbol{S}_e$ are the hole and electron spin operators, respectively. In our case the electron spin is the total angular momentum of the Ni(d^9) ion. Using the total exciton spin, $\boldsymbol{S}_{ex} = \boldsymbol{S}_h + \boldsymbol{S}_e$, the Zeeman Hamiltonian becomes

$$H_z = \mu_B g_{ex} \boldsymbol{S}_{ex} \cdot \boldsymbol{H} \tag{34}$$

where $g_{ex} = g_e + g_h$. g_e and g_h are calculated by projecting the vectors $\boldsymbol{S}_e$ and $\boldsymbol{S}_h$ onto $\boldsymbol{S}_{ex}$:

$$\begin{aligned} g_e &= g_e^{eff}(\boldsymbol{S}_e \cdot \boldsymbol{S}_{ex})/(\boldsymbol{S}_{ex} \cdot \boldsymbol{S}_{ex}) \\ g_h &= K(\boldsymbol{S}_h \cdot \boldsymbol{S}_{ex})/\boldsymbol{S}_{ex} \cdot \boldsymbol{S}_{ex}). \end{aligned} \tag{35}$$

The effective g-factor

$$g_e^{eff} = g_s + \tilde{g}_L + \Delta g_L \tag{36}$$

of the Ni($\tilde{d}^9$) electron shell includes the electron spin part, g_s, and the contribution, $\tilde{g}_L$, of the reduced electron orbital, $\tilde{L}$. The third part Δg_L arises from the spin–orbit coupling and other corrections. The value g_e^{eff} is obtained from the linear Zeeman interaction of the impurity Ni($\tilde{d}^9$) ion

$$\langle \psi(\mathrm{Ni}^+)|H_z|\psi(\mathrm{Ni}^+)\rangle = \pm\tfrac{1}{2}\mu_0 H_\parallel g_e^{eff}. \tag{37}$$

Then g_s and $\tilde{g}_L$ are calculated using the momenta $\boldsymbol{S}$ and $\tilde{\boldsymbol{L}}$ projected on the total momentum $\boldsymbol{J} = \tilde{\boldsymbol{L}} + \boldsymbol{S}$,

$$\begin{aligned} g_s &= g_0(\boldsymbol{S} \cdot \boldsymbol{J})/(\boldsymbol{J} \cdot \boldsymbol{J}) \\ \tilde{g}_L &= \gamma_r \alpha(\tilde{\boldsymbol{L}} \cdot \boldsymbol{J})/\boldsymbol{J} \cdot \boldsymbol{J}) \end{aligned} \tag{38}$$

where g_0 is the free electron g-factor.

Two main competing mechanisms can be responsible for the g-value quenching [24]. The reduction factor γ_r results from the electron–vibration interaction (Ham effect [25])

whose value for the d^9 system is given in [26] (see also [27] for review). The reduction factor α characterizes the second mechanism, i.e., the covalency effect resulting from the electron delocalization [24, 28–31]. Due to strong delocalization of the Ni($\tilde{d}^9$) electron wave function in CdS (14) the Ham effect is small as compared to the covalency effect. Although the electron–vibration interaction can be of some importance in ZnS:Ni($\tilde{d}^9$), the hybridization mechanism alone gives a correct value of g even in this case. The covalency factor α can be calculated explicitly in our model in terms of the hybridization-related parameter M' (see equations (13) and (14)).

The reduced orbital momentum, $\langle\psi(\mathrm{Ni}^+)|\boldsymbol{L}|\psi(\mathrm{Ni}^+)\rangle$ is calculated using the well known facts that its value is $\alpha_d = -1$ for a d wave function and $\alpha_p = 1$ for a p wave function [24]. Equations (37) and (13) yield

$$g^e_{eff}(\mathrm{Ni}^+) = \frac{1}{1+M'}\left\{\frac{4}{3}\alpha_d + \left(-\frac{2}{3} + 2M'\right)\right\} = 2\left(\frac{M'-1}{M'+1}\right) \tag{39}$$

for ZnS:Ni. The same calculation with the wave function (14) gives

$$g^e_{eff}(\mathrm{Ni}^+) = \frac{1}{1+M'}\left\{\frac{4}{3}(\alpha_d + \alpha_p M') - \frac{2}{3}(1+M')\right\} = \frac{2}{3}\left(\frac{M'-3}{M'+1}\right) \tag{40}$$

for CdS:Ni. Thus two different expression for the electron g-factor are obtained in the two hosts with differing lattice symmetries for the same configuration Ni($\tilde{d}^9$) of the impurity. It is emphasized that the values of the parameter M', which is function of the bound electron energy, differ for these two systems also very strongly.

The resulting exciton g-factor for ZnS:Ni becomes

$$g_{(ex)} = \tfrac{1}{2}\left(2(M'-1)/(M'+1) + K\right) + \Delta g_L. \tag{41}$$

The g-factor for the Γ_7 electron state in ZnS:Ni is known to be $g_{eff} \simeq -1.4$ [32]. To obtain this value from equation (39) one should assume that $\tilde{M}'_{\Gamma_7 v} \simeq 0.18$. This small and positive value corresponds to a deep d level in the middle of the gap which occurs in ZnS:Ni (see figure 1). Although the parameter K for the degenerate $\Gamma_7 - \Gamma_8$ valence band is not known, the authors of [5] postulate the spin-like behaviour of the acceptor state with completely quenched orbital momentum and g_h-factor around two to explain the experimental value $g_{(ex)} = 0.50$ for the deeply bound exciton in this system. They emphasize that this estimate does not work for [$\mathrm{Ni}^{(-)}(d^9)$, h] in CdS.

Unlike various d^9 systems and particularly Ni(d^9), which are known to have negative g-factors in many host semiconductors, Ni(d^9) yields a positive and large g-value in CdS. Using equation (40) for CdS:Ni and the large M'-value of $M'_{\Gamma_4 c}(E_{\Gamma_4}) \gg 1$ one arrives at $g_{eff} \simeq +2$. This large M'-value is indeed expected in a wurzite-type crystal due to the lift of the symmetry ban discussed earlier and due to proximity of the impurity Γ_4 level to the conduction band edge (see figure 2).

The g-factor of the intermediately bound exciton is described by equation

$$g_{(ex)} = \tfrac{1}{2}\left(\tfrac{2}{3}(M'-3)/(M'+1) + K\right) + \Delta g_L. \tag{42}$$

instead of (41).

As for the K-value, we believe that in a wurzite-type crystal when the above short-range potential binds the hole from the Γ_4 degenerate valence bands the assumption of a spin-like hole state works well. So the value of $K \approx +2$ seems to be reasonable for both crystals. For CdS:Ni the experimental value of 2.26 for the $g_{(ex)}$-factor indicates that $M' \gg 1$, which is in agreement with the above theoretical considerations.

5.2. Classification of the exciton levels

A simpler structure of the Ni-bound exciton spectrum in CdS as compared to that in ZnS is explained mainly by a simpler structure of the bound hole state.

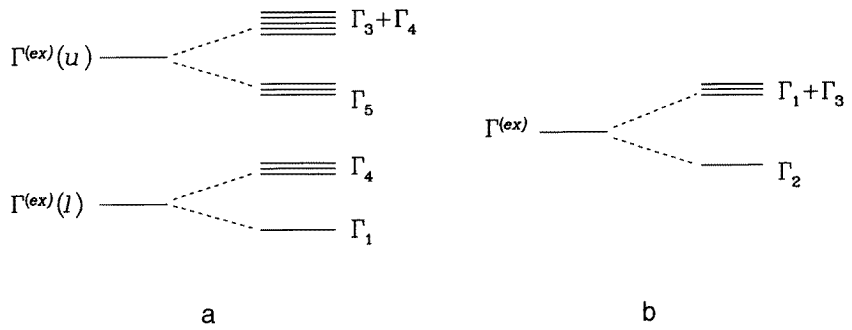

Figure 3. A schematic representation of the exciton level splitting for ZnS:Ni (a) and CdS:Ni (b).

The exciton wave functions transform according to the irreducible representation $\Gamma^{ex} = \Gamma(\mathrm{d}^{n+1}) \times \gamma_h = \Gamma_4$, which is just a direct product of the electron and hole representations $\Gamma(\mathrm{d}^{n+1}) = \Gamma_4$ (Γ_7) for CdS (ZnS).

The hole s wave function in ZnS:Ni is well described within the effective mass theory, and therefore it transforms according to the representation

$$\gamma_h(\mathrm{u}) = \Gamma_1 \times \Gamma_8 = \Gamma_8$$

or

$$\gamma_h(\mathrm{l}) = \Gamma_1 \times \Gamma_7 = \Gamma_7 \tag{43}$$

where Γ_8 and Γ_7 are the representations of the upper and the lower valence bands respectively whereas Γ_1 corresponds to the envelope s function. Using the Γ_7 representation of the $\mathrm{Ni}^+(\mathrm{d}^9)$ ground state in ZnS the exciton wave functions transform according to the representations

$$\begin{aligned} \Gamma^{(ex)}(\mathrm{u}) &= \Gamma_7 \times \Gamma_8 = \Gamma_3 + \Gamma_4 + \Gamma_5 \\ \Gamma^{(ex)}(\mathrm{l}) &= \Gamma_7 \times \Gamma_7 = \Gamma_1 + \Gamma_4. \end{aligned} \tag{44}$$

Due to the exchange interaction the upper exciton level splits into a triplet, Γ_5, and quintet, $\Gamma_3 + \Gamma_4$, and the lower one splits into a triplet, Γ_4, and singlet, Γ_1.

The pattern obtained here is standard for excitons in which the second carrier is bound by a Coulomb field of the first one in hydrogen-like states. Accounting for the higher hydrogen-like states more levels with more complicated structure are expected.

In the case of the intermediate-radius e–h pair in CdS:Ni the ground state of the hole is formed by the short-range pseudopotential (20) with the projection operator $\hat{P}_{\Gamma_4}$ built in. Therefore, its wave functions transform according to the representation Γ_4.

The Γ_4 representation of the $\mathrm{Ni}^+(\mathrm{d}^9)$ ground state in CdS:Ni gives a

$$\Gamma^{(ex)} = \Gamma_4 \times \Gamma_4 = \Gamma_1 + \Gamma_2 + \Gamma_3 \tag{45}$$

representation for the exciton bound state. The exchange interaction splits this level into a singlet, Γ_2, and a triplet, $\Gamma_1 + \Gamma_3$. The latter state was observed experimentally in [5]. The Γ_2 level does not show up in this experiment since the Γ_2–Γ_4 dipole transitions are symmetry forbidden.

Hydrogen-like bound hole states are also possible but these should be looked for very close to the charge transfer edge band with very small binding energy as a result of the Coulomb potential weakness.

5.3. Bound exciton energy

Now we return to the problem of the exciton binding energy. The energy which is required to form acceptor excitons bound to transition metal impurities (2) can be represented as

$$E_{bex} = E_i(0/-) + E_h.$$

The energy E_{bex} is directly determined from optical experiments. However, the electron ionization energy, $E_i(0/-)$, can be found only from a numerical fit of the charge transfer bands to some theoretical curve describing the ionization cross-section near the threshold.

The exciton hole energy in CdS was found to be about 140 meV [5]. This energy should be compared with that for ZnS, but different measurements gave differing results for this system. The first numerical data for ZnS:Ni were presented by Kazanskii and Ryskin [23], who estimated the exciton hole binding energy as ≈ 170 meV. Later Noras and Allen [8] extracted the value of $E_{v0} \approx 20$ meV from their optical absorption measurements. The recent data of Heitz *et al* [5] gave $E_{v0} = 108$ meV. The difference in the results is due to the different methods used to derive the ionization energy, $E_i(0/-)$.

The well known method of processing the experimental data is by using a Lucovsky-type law for the threshold behaviour of absorption coefficient $\alpha \sim (\hbar\omega - E_i)^n$. Noras and Allen have chosen $n = \frac{3}{2}$ whereas Heitz *et al* [5] used a method based on the investigation of the energy transfer processes between different transition metal centres by excitation spectroscopy. In both cases the $n = \frac{1}{2}$ characteristic of the allowed dipole transitions is neglected. From the theoretical point of view the photoionization reaction $Ni^{2+}(e^4t_2^4) \rightarrow Ni^{+}(e^4t_2^5) + h_p$ should contain both allowed and forbidden components [33] because the ninth t_2 electron wave function consists of the d and p partial waves in accordance with equation (13), thus a component with $n = \frac{1}{2}$ should also be taken into account. Although the recent data show that the hole binding energy seems to be larger for the Ni-bound hole in CdS than for that in ZnS, the information available is still contradictory. In any case, we conclude from the above discussion that there are many sources of violation of the simple hydrogen-like estimation of the acceptor energy (which is estimated to be $\simeq$170 meV in ZnS [3])). Some of these mechanisms are common for ZnS and CdS.

6. Summary

We have found that there are reasons for introducing the intermediately bound exciton concept at least in the case of CdS:Ni, although one should not speak literally about a neutral $Ni^{(2+)}$ ion capturing a loosely bound electron and hole. We have seen that the difference between the bound exciton states in zinc blende ZnS:Ni and wurzite CdS:Ni systems is first of all due to the lower symmetry of the latter crystal. It is also important that the relevant impurity deep level is close enough to the bottom of the conduction band. Only then does the enhancement of the d–s hybridization play a really important part.

The structures of the bound exciton wave functions in the two cases are strongly at variance. The tetrahedral system ZnS:Ni is characterized by standard excitons bound to the transition metal impurity as described, e.g., in review [3]. The electron is bound in a strongly localized d state while the hole is loosely bound by the Coulomb field of the electron.

Intermediately bound excitons are typical for the hexagonal system CdS:Ni. The wave function of the ninth electron of the Ni($\tilde{d}^9$) pseudoion is swollen strongly due to the hybridization of the d states with the Bloch states at the bottom of the conduction band. The hole is bound by the short-range pseudopotential, which has properties of a Γ_7 projection operator. In contrast to the zinc blende system the Coulomb potential of the ninth electron is less important and may result only in small corrections.

The importance of the proximity of the deep levels to the bottom of the conduction band can be seen for examples in the systems like CdS:Cu and the wurzite phase of ZnS doped by Ni. In both systems the relevant deep level lies rather far from the conduction band and intermediate bound excitons do not appear. However, these excitons are clearly seen in ZnO:Cu (detailed discussion of the properties of this system will be published elsewhere).

The most important manifestation of the differences between ZnS:Ni and CdS:Ni is completely different values of the exciton g-factors, which are now readily explained by the different localization and symmetries of the exciton wave functions. The differences in the Zeeman spectra are also accounted for by the same mechanism. We should mention also the shift of the binding energy of the CdS:Ni exciton as well as some other physical properties of these systems which can be understood within our model.

There are various consequences of this model which can be checked experimentally. One of these can be mentioned here. The principal point of the model is the appearance of the s–d hybridization with the conduction band states in low-symmetry crystals. This makes us think that, being able to induce a transition from a tetrahedral to a hexagonal lattice, say, by a strong enough uniaxial pressure, we will be also able to convert an exciton bound deeply to a transition metal impurity into an intermediate one with corresponding changes of its spectral features. Observation of such a transition would be considered as a direct test of the model.

Appendix. The electron part

Here the Bloch tail

$$\sqrt{\tilde{M}'_{v\Gamma_5}}\psi_{bt_2} = \sum_{\boldsymbol{k}a\sigma} \frac{\langle t_2\mu|U'|\boldsymbol{k}\tilde{a}\sigma\rangle}{E_{\boldsymbol{k}a\sigma} - E_i}\tilde{\psi}_{\boldsymbol{k}a\sigma} \tag{A1}$$

of the impurity wave function (11) is calculated. Assuming that the main contribution is from the vicinity of the Γ point of the band a (valence or conduction) allows one to use the following approximation. It is assumed that

$$\langle a\mathrm{t}_2\mu|W|\boldsymbol{k}\tilde{a}\sigma\rangle \approx V_{at_2}.$$

The basis of the orthogonalized Bloch functions, $\tilde{\psi}_{\boldsymbol{k}a}$ is substituted by the set of Kohn–Luttinger functions $\tilde{\chi}_{\boldsymbol{k}a}(\boldsymbol{r}) = \tilde{u}_{0a}(\boldsymbol{r})\exp(-\mathrm{i}\boldsymbol{k}\cdot\boldsymbol{r})$ with the Bloch amplitude at $\boldsymbol{k} = 0$

$$\tilde{u}_{0a}(\boldsymbol{r}) = u_{0a}(\boldsymbol{r}) - \sum_{\gamma\mu}\langle\gamma\mu|u_{0a}\rangle\psi_{\gamma\mu}$$

orthogonalized to the core states.

As a result the tail wave function reads

$$\sqrt{\tilde{M}'_{a\Gamma_5}}\psi_{bt_2} \simeq (a_0)^3\sum_a(\pm)\tilde{V}_{at_2}\sum_{\boldsymbol{k}}\frac{\exp(-\mathrm{i}\boldsymbol{k}\cdot\boldsymbol{r})}{|E_{\Gamma_7} - E_{0a}| + \hbar k^2/2m_a^*}\tilde{u}_{oa}(\boldsymbol{r}) \tag{A2}$$

the $+$ or $-$ signs appearing if the contribution originates from the conduction or a valence band respectively.

Replacing summation over $\boldsymbol{k}$ by an integration yields

$$\sqrt{\tilde{M}'_{a\Gamma_5}}\psi_{bt_2} \simeq (a_0)^3 \sum_a (\pm)\tilde{V}_{at_2}\frac{2m^*}{\hbar^2}\frac{\tilde{u}_{0a}(\boldsymbol{r})}{4\pi}\frac{\mathrm{e}^{-k_a r}}{r}. \tag{A3}$$

where $k_a^2 = (2m^*\Delta_{\Gamma_7}/\hbar^2)$ and $\Delta_{\Gamma_7} = |E_{\Gamma_7} - E_{0a}|$. This tail function could be presented as

$$\sqrt{\tilde{M}'_{a\Gamma_5}}\psi_{bt_2} \simeq \sum_a (\pm)\left(\frac{a_0}{a_\Gamma}\right)^3 \frac{1}{4\pi}\frac{\tilde{V}_{at_2}}{\Delta_\Gamma}\tilde{u}_{0a}\frac{\mathrm{e}^{-k_a r}}{k_a r} \tag{A4}$$

where $\tilde{V}_{at_2}$ is a typical value of the hybridization with the band a.

The normalized wave function of the tail part is

$$\sqrt{\tilde{M}'_{a\Gamma_5}}\psi_{bt_2} = \sum_a (\pm)\frac{\tilde{V}_{at_2}}{\Delta_\Gamma}\varphi_a(r) \tag{A5}$$

where

$$\varphi_a(r) = \left(\int \left|\tilde{u}_{0a}(\boldsymbol{r})\frac{\mathrm{e}^{-k_a r}}{k_a r}\right|^2 \mathrm{d}^3 r\right)^{-1/2} \tilde{u}_{0a}(\boldsymbol{r})\frac{\mathrm{e}^{-k_a r}}{k_a r}.$$

References

[1] Hopfield J J, Thomas D G and Lynch R T 1966 *Phys. Rev. Lett.* **17** 312
[2] Fleurov V N and Kikoin K A 1982 *Solid State Commun.* **42** 353
[3] Sokolov V I and Kikoin K A 1989 *Sov. Sci. Rev.* A **12** 149
[4] Kikoin K N and Fleurov V N 1994 *Transition Metal Impurities in Semiconductors. Electronic Structure and Physical Properties* (Singapore: World Scientific) p 349
[5] Heitz R, Hoffmann A and Broser I 1993 *Phys. Rev.* B **48** 8672
[6] Heitz R, Hoffmann A, Thurian P and Broser I 1992 *J. Phys.: Condens. Matter* **4** 157
[7] Peka P and Schultz H-J 1994 *Solid State Commun.* **89** 225
[8] Noras J M and Allen J W 1980 *J. Phys. C: Solid State Phys.* **13** 3511
[9] Dahan P, Fleurov V and Kikoin K 1995 *Mater. Sci. Forum* **196–201** 755
[10] Kikoin K A and Fleurov V N 1981 *Sov. Phys.–JETP* **50** 535
[11] Bishop S G, Robbins D J and Dean P J 1980 *Solid State Commun.* **33** 119
[12] Robbins D J, Dean P J, West C L and Hayes W 1982 *Phil. Trans. R. Soc.* **304** 499
[13] Kikoin K A, Sokolov V I, Fleurov V N and Chernyaev V V 1982 *Sov. Phys.–JETP* **56** 1354
[14] Zunger A 1986 *Solid State Physics*, vol 39, ed H Ehrenreich and D Turnbull (Orlando, FL: Academic) p 276
[15] Haldane F D M and Anderson P W 1976 *Phys. Rev.* B **13** 2553
[16] Fleurov V N and Kikoin K A 1976 *J. Phys. C: Solid State Phys.* **9** 1673
[17] Kikoin K A and Fleurov V N 1977 *J. Phys. C: Solid State Phys.* **10** 4295
[18] Picoli G, Chomette A, and Lannoo M 1984 *Phys. Rev.* B **30** 7138
[19] Cho K 1979 *Excitons (Topics in Current Physics)* (Berlin: Springer)
[20] Pantelides S T 1978 *Rev. Mod. Phys.* **50** 797
[21] Harrison W A 1970 *Solid State Theory* (New York: McGraw-Hill)
[22] Perel' V I and Yassiyevich I N 1982 *Sov. Phys.–JETP* **55** 143
[23] Kazanskii and Ryskin 1971 *Sov. Phys.–Solid State* **13** 3153
[24] Abragam A and Bleaney B 1970 *Electron Paramagnetic Resonance of Transition Ions* (Oxford: Clarendon)
[25] Ham F S 1965 *Phys. Rev.* A **148** 1727
[26] Clerjaud B and Gelineau A 1974 *Phys. Rev.* B **9** 2832
[27] Bates C A 1978 *Phys. Rep.* C **35** 187
[28] Watts R K 1969 *Phys. Rev.* **188** 568
[29] Yamaguchi T and Kamimura H 1972 *J. Phys. Soc. Japan* **33** 953
[30] Kaufmann U, Koschel W H, Schneider J and Weber J 1979 *Phys. Rev.* B **19** 3343
[31] Katayama-Yoshida H 1987 *Int. J. Mod. Phys.* **1** 1207
[32] Clerjaud B, Gelineau A, Gendron F, Porte C, Baranowski J M and Liro Z 1984 *J. Phys. C: Solid State Phys.* **17** 3837
[33] Fleurov V N and Kikoin K A 1982 *J. Phys. C: Solid State Phys.* **15** 3523